Effects of MeV Si ions bombardment on the thermoelectric generator from SiO$_2$/SiO$_2$ + Cu and SiO$_2$/SiO$_2$ + Au nanolayered multilayer films

S. Budak [a,*], J. Chacha [a], C. Smith [b,c], M. Pugh [a], T. Colon [d], K. Heidary [a], R.B. Johnson [c], D. Ila [b,c]

[a] Department of Electrical Engineering, Alabama A&M University, Normal, AL, USA
[b] Center for Irradiation of Materials, Alabama A&M University, Normal, AL, USA
[c] Department of Physics, Alabama A&M University, Normal, AL, USA
[d] Department of Mechanical Engineering, Alabama A&M University, Normal, AL, USA

ARTICLE INFO

ABSTRACT

The defects and disorder in the thin films caused by MeV ions bombardment and the grain boundaries of these nanoscale clusters increase phonon scattering and increase the chance of an inelastic interaction and phonon annihilation. We prepared the thermoelectric generator devices from 100 alternating layers of SiO$_2$/SiO$_2$ + Cu multi-nano layered superlattice films at the total thickness of 382 nm and 50 alternating layers of SiO$_2$/SiO$_2$ + Au multi-nano layered superlattice films at the total thickness of 147 nm using the physical vapor deposition (PVD). Rutherford Backscattering Spectrometry (RBS) and RUMP simulation have been used to determine the stoichiometry of the elements of SiO$_2$, Cu and Au in the multilayer films and the thickness of the grown multi-layer films. The 5 MeV Si ions bombardments have been performed using the AAMU-Center for Irradiation of Materials (CIM) Pelletron ion beam accelerator to make quantum (nano) dots and/or quantum (quantum) clusters in the multilayered superlattice thin films to decrease the cross plane thermal conductivity, increase the cross plane Seebeck coefficient and cross plane electrical conductivity. To characterize the thermoelectric generator devices before and after Si ion bombardments we have measured Seebeck coefficient, cross-plane electrical conductivity, and thermal conductivity in the cross-plane geometry for different fluences.

© 2011 Elsevier B.V. All rights reserved.

1. Introduction

Thermoelectrics have been investigated for their cooling and energy harvesting uses over the last six decades. Those devices can be brought from a number of commercial suppliers [1]. In recent decades, as the world's demand for exploiting new energy conversion materials increases, continuing interests have being focused on thermoelectric (TE) materials because of their clean and sustainable energy converting characteristics [2]. The technology of thermoelectricity began during the World War II when Soviet Union, under the Academician Ioffe's inspiration, produced 2–4 watt thermoelectric generators to be capable of powering a small radio from a small cooking fire [3]. Solid-state thermoelectric (TE) cooling and electrical power generation devices have many attractive features compared with other methods of refrigeration or electrical power generation, such as long life, no moving parts, and no emissions of toxic gases, low maintenance, and high reliability [4].

Thermoelectric materials with the high figure of merit can enable novel thermoelectric and thermionic devices with efficient solid-state refrigeration and power conversion. In recent years, there has been a considerable interest in exploiting the thermoelectric properties of low-dimensional structures, such as quantum well, superlattices, and one dimensional wire [5]. The central issue in thermoelectrics research is to increase thermoelectric figure of merit ZT. The best thermoelectric materials were succinctly summarized as "phonon-glass electron crystal" (or PGEC in short), which means that the materials should have a low lattice thermal conductivity as in glass, and a high electrical conductivity as in crystals [6]. Low dimensional materials, such as quantum wells, superlattices, quantum wires, and quantum dots offer new ways to manipulate the electron and phonon properties of a given material [7]. Thermoelectric devices are basically categorized into two groups on the direction of energy conversion: thermoelectric cooler (TEC) converting electricity to thermal energy and thermoelectric generator (TEG) converting heat into electricity [8]. The efficiency of the thermoelectric devices and materials is determined by the figure of merit ZT [9]. The figure of merit is defined by $ZT = S^2\sigma T/\kappa$, where S is the Seebeck coefficient, σ is the electrical conductivity, T is the absolute temperature, and κ is the thermal conductivity [10,11]. ZT can be increased by increasing S, by

* Corresponding author. Tel.:+1 256 372 5894; fax: +1 256 372 5855.
E-mail addresses: satilmis.budak@aamu.edu (S. Budak), chacha_john79@hotmail.com (J. Chacha), cydale@cim.aamu.edu (C. Smith), marcuspughp@yahoo.com (M. Pugh), kaveh.heidary@aamu.edu (K. Heidary), barry@w4wb.com (R.B. Johnson), ila@cim.aamu.edu (D. Ila).

increasing σ, or by decreasing κ. In this study we have reported on the growth of $SiO_2/SiO_2 + Cu$ and $SiO_2/SiO_2 + Au$ multi-layer super-lattice films using PVD, and high energy Si ions bombardment of the films for reducing thermal conductivity and increasing both electrical conductivity and Seebeck coefficient in the cross plane geometry. We have published the preliminary results of the current study of $SiO_2/SiO_2 + Cu$ thin films in Ref. [12].

2. Experimental

We have deposited the 100 alternating layers of $SiO_2/SiO_2 + Cu$ nano-layers films and 50 alternating layers of $SiO_2/SiO_2 + Au$ multi-nano layered superlattice on silicon and silica (fused quartz) substrates at the total thickness of 382 and 147 nm respectively using the physical vapor deposition (PVD). The multilayer films of $SiO_2/SiO_2 + Cu$ were sequentially deposited to have a periodic structure consisting of alternating SiO_2 and $SiO_2 + Cu$ layers, and the multilayer films of $SiO_2/SiO_2 + Au$ were sequentially deposited to have a periodic structure consisting of alternating SiO_2 and $SiO_2 + Au$ layers. The two electron-gun evaporators were turned on and off alternately to make multilayers. The base pressure in PVD chamber during the deposition was about 5×10^{-6} Torr. The growth rate was monitored by a gold coated Inficon Quartz Crystal Monitor (QCM). In the PVD system, we have used e-beam, and we have expected to see amorphous thin films. We made substrate holder rotate during the deposition, by this way we could reach much better quality thin film systems. Since we did not have XRD results due to not having this facility, we could not say the crystal structure of the film systems. The film geometries used for deposition of $SiO_2/SiO_2 + Cu$ nano-layers films are shown in Fig. 1a and b for the cross plane thermal conductivity and for the cross plane Seebeck coefficient and the cross plane electrical conductivity measurements respectively. The film geometries used for deposition of $SiO_2/SiO_2 + Au$ nano-layers films are shown in Fig. 2a and b for the thermal conductivity and for Seebeck coefficient measurements respectively. The cross plane electrical conductivity was measured by the 4-probe contact system and the cross plane thermal conductivity was measured by the home-made 3ω (3rd harmonic) technique. The cross plane Seebeck coefficient was measured using MMR Technologies Seebeck system. The electrical conductivity, thermal conductivity and Seebeck coefficient measurements have been performed at room temperature. De-
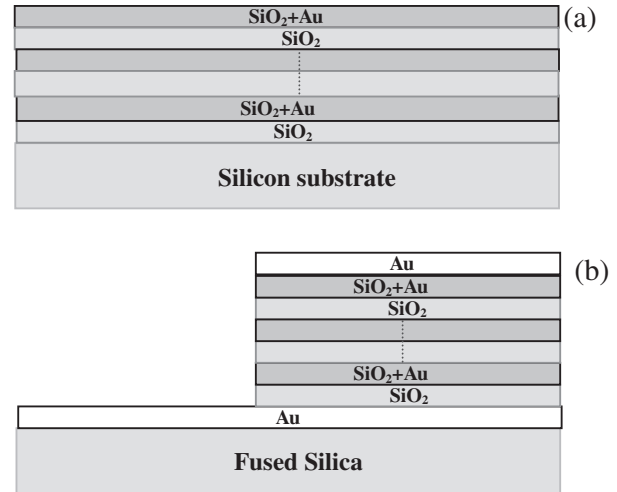
tailed information about the 3ω technique might be found in Refs. [13–15]. In order to make nano-clusters and/ or nano-dots in the layers, 5 MeV Si ions bombardments were performed with the Pelletron ion beam accelerator at the Alabama A&M University Center for Irradiation of Materials (AAMU-CIM). The Stopping and Range of Ions in Matter software (SRIM) was used to choose the suitable energy for bombarding the samples with MeV Si ions. The fluences used for the bombardment were between 1×10^{12} and 1×10^{14} ions/cm^2 for the two different thin film systems. Rutherford Backscattering Spectrometry (RBS) was performed using 2.1 MeV He$^+$ ions with the particle detector placed at 170° from the incident beam to monitor the film thickness and stoichiometry before and after 5 MeV Si ion bombardments [16,17].

3. Results and discussion

Fig. 3 shows the He RBS spectrum of $SiO_2/SiO_2 + Cu$ multilayer thin film prepared on Glassy Polymeric Carbon (GPC) substrate since GPC is suitable material for RBS measurements. As seen from the Fig. 2, the used materials in $SiO_2/SiO_2 + Cu$ thin film deposition

Fig. 2. Geometry of sample from the cross-section, (a) for thermal conductivity, (b) for Seebeck measurements.
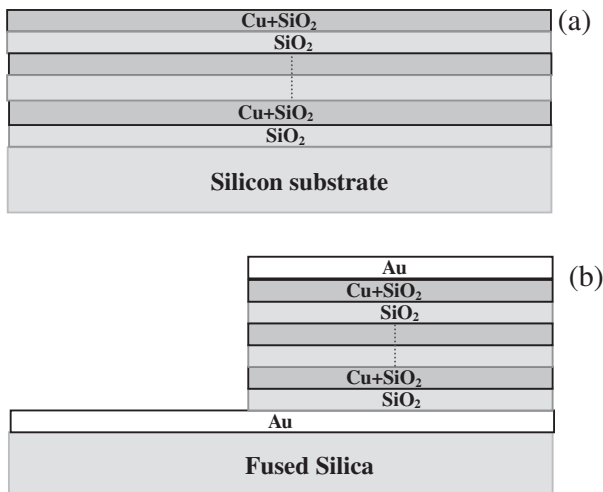
Fig. 1. Geometry of the prepared sample from the cross-section, (a) For the cross plane thermal conductivity, (b) for the cross plane Seebeck and Electrical Conductivity measurements.
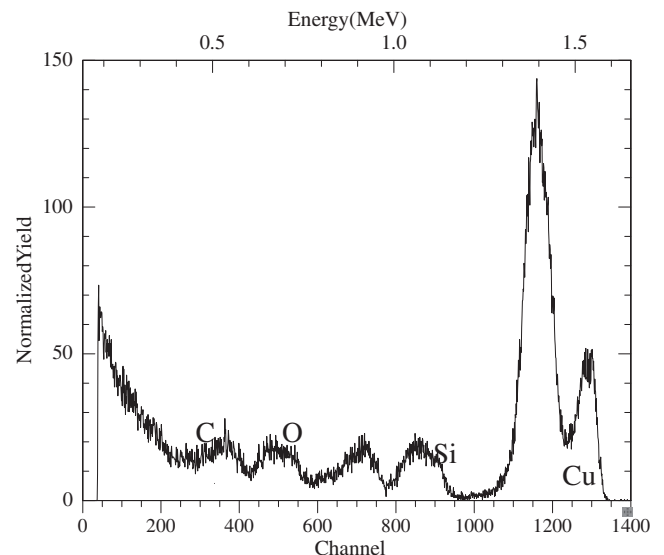
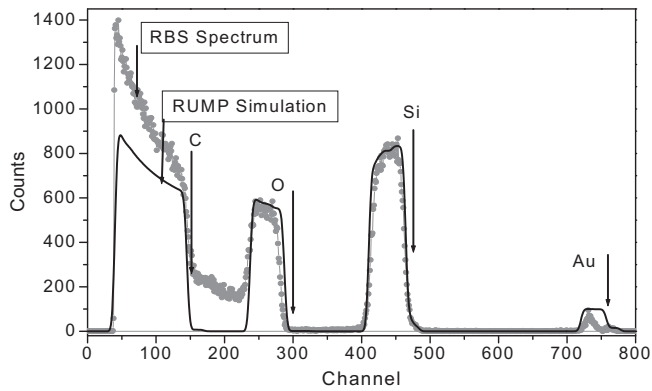**Fig. 3.** He RBS spectrum of $SiO_2/SiO_2 + Cu$ multilayer film on GPC substrate.

Fig. 4. He+ RBS spectrum and RUMP simulation for SiO_2/SiO_2 + Au nano-layered films on GPC substrate.

and the energy correspondence of the channels of the elements have been shown on the RBS spectrum. After the suitable optimizations depending on the figure of merit results could be done on the elemental analysis of the SiO_2/SiO_2 + Cu multilayer thin films, the more suitable thin films for the higher efficient device fabrications could be produced in our future studies.

Fig. 4 shows RBS spectrum and RUMP simulation of 50 alternating layers of SiO_2/SiO_2 + Au films on a Glassy Polymeric Carbon (GPC) substrate when the sample is at the normal angle. The same stoichiometry was kept for our 50 alternating layer film deposition on the silicon and silica substrates for the thermoelectric generator fabrication. RUMP simulation [18] was used both to specify the average thickness of 50 layers for SiO_2/SiO_2 + Au co-deposited layers as 147 nm and the elemental analysis of the thin films.

Fig. 5 shows the thermoelectric properties of 100 alternating layers of SiO_2/SiO_2 + Cu virgin and 5 MeV Si ions bombarded thin films at five different fluences. Fig. 5a shows the square of the cross plane Seebeck coefficient of the thin films. Since electrons are the main charge carriers in our deposited SiO_2/SiO_2 + Cu thin film systems, the original cross plane Seebeck values are negative. The virgin (unbombarded) sample has Seebeck coefficient of −40.31 μV/K and this value changed to −22.59 μV/K at the fluence of 1×10^{12} ions/cm²; −67.82 μV/K at the fluence of 5×10^{12} ions/cm² and reached the value of -135.32 μV/K at the fluence of 1×10^{13} ions/cm²; −345.79 μV/K at the fluence of 1×10^{12} ions/cm², and −339.62 μV/K at the fluence of 1×10^{14} ions/cm². The increase in the negative side of the cross plane Seebeck coefficients is one of the expected things for the high efficient thermoelectric materials and devices. These results in the Seebeck coefficient showed that the 5 MeV Si ions beam bombardments have modified the microstructure of the SiO_2/SiO_2 + Cu multilayer thin films and it has caused an increase in the cross plane Seebeck coefficient at almost applied fluences.

As seen from Fig. 5b, the *remarkable* increase in the cross plane electrical conductivity was observed until the fluence of 5×10^{13} ions/cm². After the fluence of 5×10^{13} ions/cm², the cross plane electrical conductivity value started to decrease. The increase in the electrical conductivity is one of the other expected things for the high efficient thermoelectric materials and devices. Until the fluence of 5×10^{13} ions/cm², the introduced fluences of the MeV Si ions were suitable to increase the electrical conductivity. Fig. 5c shows that the cross plane thermal conductivity value started to decrease when the first ion bombardment was introduced at the fluence of 1×10^{12} ions/cm². The decrement in the thermal conductivity continued to the fluence of 5×10^{12} ions/cm². After the fluence of 5×10^{12} ions/cm², the cross plane thermal conductivity showed an increase until the fluence of 1×10^{13} ions/cm². After the fluence of 5×10^{13} ions/cm², the cross

plane thermal conductivity decreased and increased depending on the applied fluences. The MeV Si ions bombardments at the different fluences affected the thermal conductivity values in the positive direction since the thermal conductivity values decreased when the fluences were started. The decrease in the thermal conductivity is one of the other expected values for the high efficient thermoelectric materials and devices. The 5 MeV Si ions beam modified the thin film systems, and the nano-cluster and/or nano-dots formation due to the ion beam bombardments caused the decrease in the cross plane thermal conductivity values. Finally, we have calculated the figure of merit ZT before and after 5 MeV Si ions bombardments as shown in Fig. 5d. The desired result of ion bombardment on ZT strongly appears until the fluence of 5×10^{13} ions/cm². ZT reached 0.057 at the fluence of 5×10^{13} ions/cm². This result is very remarkable for the preliminary studies of SiO_2/SiO_2 + Cu superlattice thin film systems. The MeV Si ions beam modified the thin film systems and caused the increase in both the cross plane Seebeck coefficient and electrical conductivity, and decrease in the cross plane thermal conductivity, thus increases in ZT at the suitable fluences.

Fig. 6 shows the Seebeck coefficient temperature dependence of SiO_2/SiO_2 + Au multilayer films at different fluences. As seen from Fig. 6, the MeV Si ions bombardments showed positive effects on the Seebeck coefficient. Seebeck coefficient of the sample depending on the temperature at the different fluences showed an increment in the negative axis direction since the sample has the charge carriers of electrons. Seebeck coefficient measurements showed n-type behavior for SiO_2/SiO_2 + Au multilayer thin films. As seen from
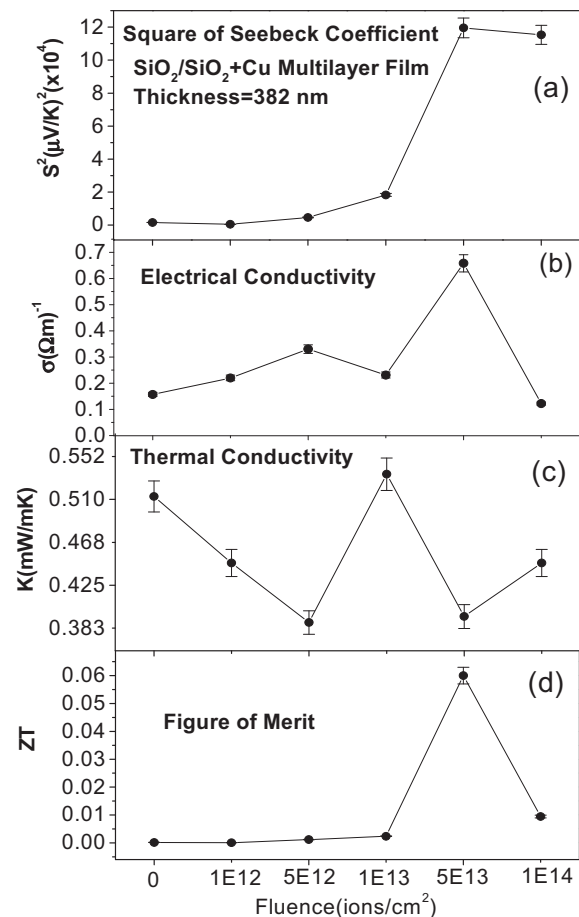

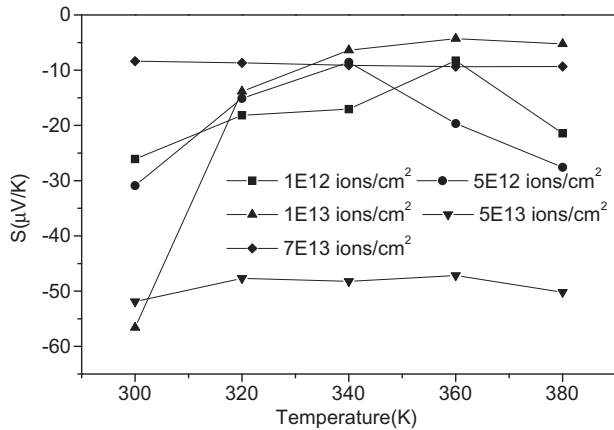**Fig. 5.** Thermoelectric properties of 100 alternating nanolayers of SiO_2/SiO_2 + Cu multilayer films.

Fig. 6. Seebeck coefficient temperature dependence of $SiO_2/SiO_2 + Au$ multilayer films at different fluences.

Fig. 6, the maximum effect could be seen at the room temperature bombarded at the fluence of 1×10^{13} ions/cm^2. Generally speaking, the maximum effect occurred at the fluence of 5×10^{13} ions/cm^2 for $SiO_2/SiO_2 + Au$ multilayer system while the temperature is being increased.

Fig. 7 shows the Raman analysis of $SiO_2/SiO_2 + Au$ amorphous multilayer films at different fluences. Dilor-JOBIN YVON-SPEX Raman spectrometer was used to analyze the multilayer films for order of the system and the bonds among the introduced elements in the multilayer systems. As seen from Fig. 7, the broad feature starting at around 950 cm^{-1} is an amorphous material and is laying at the subsurface of the thin film. Au does exhibit a band in this region of the Raman shift. The Au thin film deposited on glass shows a very weak Raman spectrum and Raman Spectrum indicates that Au no real contribution to the overall Raman features [19,20].

Fig. 8 shows the thermoelectric properties of 50 alternating layers of $SiO_2/SiO_2 + Au$ virgin and 5 MeV Si ion bombarded thin films at five different fluences. Fig. 8a shows the square of the Seebeck coefficient of the thin films. The original Seebeck values are negative that is, we have negative thermo-power and electrons are the main charge carriers. The virgin sample has Seebeck coefficient of -40.81 μV/K at the room temperature and this value decreased from this value until maximum value of -56.49 μV/K at the fluence
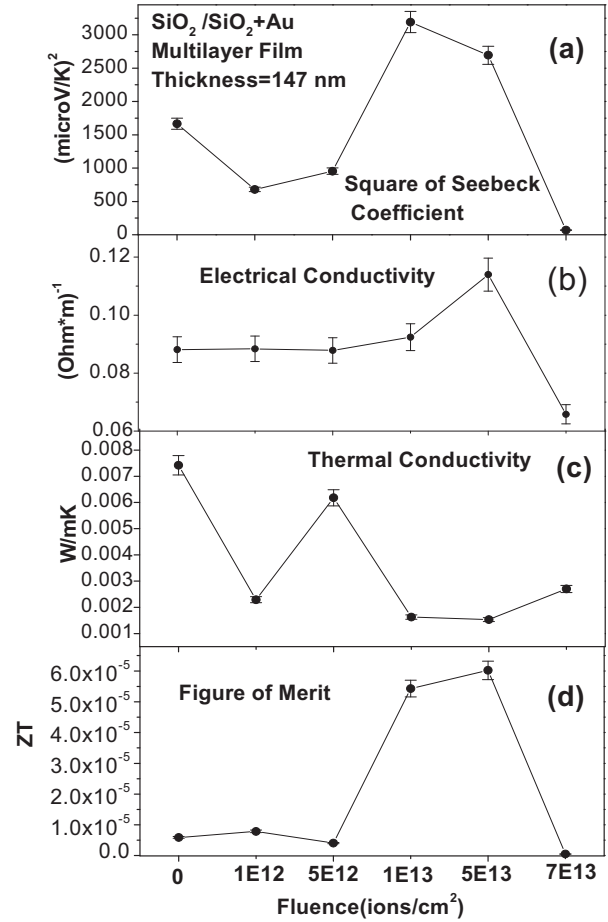

Fig. 8. Thermoelectric properties of 50 alternating nanolayers of $SiO_2/SiO_2 + Au$ multilayer films.

of 1×10^{13} ions/cm^2. When MeV Si ions bombardment was continued at the increasing fluences at the room temperature, the Seebeck coefficient reached -51.9 μV/K and -8.37 μV/K at the fluences of 5×10^{13} and 7×10^{13} ions/cm^2, respectively. The observed effects of Si ions bombardment have the opposite characteristics for the electrical and the thermal conductivity values as
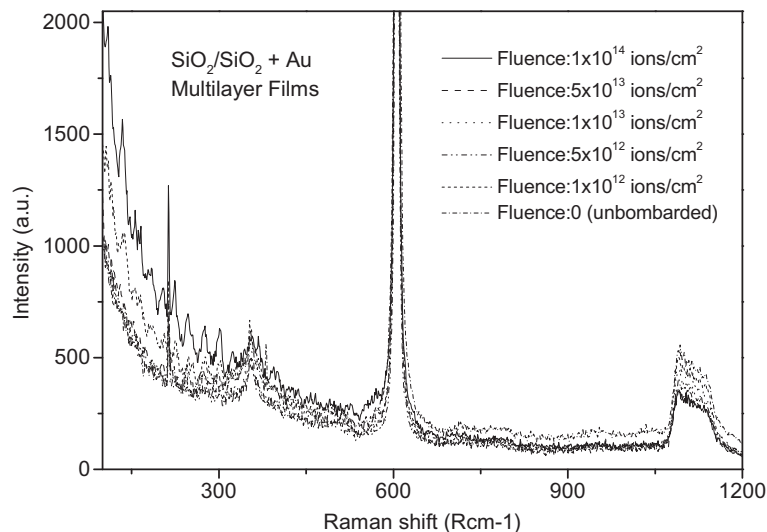

Fig. 7. Raman analysis of $SiO_2/SiO_2 + Au$ multilayer films at different fluences.

function of varying fluence, as shown in the Fig. 8b and c, respectively. As seen from Fig. 8b, the remarkable increase in the electrical conductivity was observed at the fluence of 5×10^{13} ions/cm². As seen from Fig. 8c, the thermal conductivity value decreased when the first ion bombardment was introduced at the fluence of 1×10^{12} ions/cm². After this fluence, the thermal conductivity showed an increase until the fluence of 5×10^{13} ions/cm². The turning point for the thermal conductivity is the fluence of 5×10^{12} ions/cm². After this fluence, the thermal conductivity decreased until the fluence of 5×10^{13} ions/cm². After the fluence of 5×10^{13} ions/cm², the thermal conductivity showed an increase. Fig. 8d shows ZT values. The desired result of ion bombardment on ZT strongly appears at the fluences of 1×10^{13} and 5×10^{13} ions/cm². When we consider the experimental uncertainty, we are able to say that the total effect of bombardment do not differ the ZT values for other fluences except for the fluences of 5×10^{13} and 5×10^{13} ions/cm².

4. Conclusion

We have observed the positive effects of the 5 MeV Si ions bombardments on both the thermoelectric properties of the $SiO_2/SiO_2 + Cu$ and $SiO_2/SiO_2 + Au$ superlattice multilayer thin film systems. We have been working on the different superlattice thin film systems like $SiO_2/SiO_2 + Au$, $SiO_2/SiO_2 + Ag$ as shown in Refs. [9,11], respectively. This was the first time for us to start with the $SiO_2/SiO_2 + Cu$ superlattice thin film systems. We have reached the positive effects of the 5 MeV Si ions beam modifications on the thermoelectric properties of the $SiO_2/SiO_2 + Cu$ superlattice thin film systems since the thermal conductivity values decrease while the Seebeck coefficient and electrical conductivity values increase under the effect of the MeV Si ions bombardments at the suitable fluences. The data of $SiO_2/AuSiO_2$ alternating layers clearly show that the thermoelectric properties are positively impacted at the suitable fluences. The properties quickly degrade or demonstrate limited response at some fluences as increasing fluence. This behavior suggests ion straggling or damage due to the increasing fluence. We have reported similar study as shown in Ref. [9]. Our purpose is to improve the figure of merit for the $SiO_2/SiO_2 + Cu$ and $SiO_2/SiO_2 + Au$ superlattice multilayer thin film systems. We will be continuing our investigation progress to understand the $SiO_2/SiO_2 + Cu$ and $SiO_2/SiO_2 + Au$ superlattice thin film systems at the different conditions like different thickness, different fluences and energies, different number of periods to reach more efficient thermoelectric device fabrications.

References

[1] Mehmet Arik, Jim Bray, Stanton Weaver, Proc. of SPIE 7679 (2010). 76791F-1-18.
[2] Zhen Xiong, Xihong Chen, Xueying Zhao, Shengqiang Bai, Xiangyang Huang, Lidong Chen, Solid State Sci. 11 (2009) 1612–1616.
[3] Tao Li, Guangfa Tang, Guangcai Gong, Guangqiang Zhang, Nianping Li, Lin Zhang, Appl. Therm. Eng. 29 (2009) 2016–2021.
[4] T.C. Harman, P.J. Taylor, M.P. Walsh, B.E. LaForge, Science 297 (2002) 2229–2232.
[5] J.L. Liu, A. Khitun, K.L. Wang, T. Borca-Tasiuc, W.L. Liu, G. Chen, D.P. Yu, J. Cryst. Growth 227–228 (2001) 1111–1115.
[6] G. Slack, in: D.M. Rowe (Ed.), CRC Handbook of Thermoelectrics, CRC Press, USA, 1995, pp. 407–440.
[7] T.M. Trit (Ed.), Semiconductor and Semimetals 71 (2001).
[8] C. Cheng, S. Huang, T. Cheng, Int. J. Heat Mass Transfer 53 (2010) 2001–2011.
[9] S. Budak, C. Muntele, B. Zheng, D. Ila, Nucl. Instrum. Methods B 261 (2007) 1167.
[10] S. Guner, S. Budak, R.A. Minamisawa, C. Muntele, D. Ila, Nucl. Instrum. Methods B 266 (2008) 1261.
[11] S. Budak, S. Guner, R.A. Minamisawa, D. ILA, Surf. Coat. Technol. 203 (2009) 2479–2481.
[12] J. Chacha, S. Budak, C. Smith, M. Pugh, K. Ogbara, K. Heidary, R.B. Johnson, C. Muntele, D. ILA, Mater. Res. Soc. Symp. Proc. Vol. 1267 © 2010 Materials Research Society 1267-DD05-15.
[13] L.R. Holland, R.C. Smith, J. Appl. Phys. 37 (1966) 4528.
[14] D.G. Cahill, M. Katiyar, J.R. Abelson, Phys. Rev. B 50 (1994) 6077.
[15] T.B. Tasciuc, A.R. Kumar, G. Chen, Rev. Sci. Instrum. 72 (2001) 2139.
[16] J.F. Ziegler, J.P. Biersack, U. Littmark, The Stopping Range of Ions in solids, Pergamon Press, New York, 1985.
[17] W.K. Chu, J.W. Mayer, M.-A. Nicolet, Backscattering Spectrometry, Academic Press, New York, 1978.
[18] L.R. Doolittle, M.O. Thompson, RUMP, Computer Graphics Service, 2002.
[19] S. Nie, S.R. Emory, Science 275 (1997) 1102.
[20] G.V. Pavan Kumar, S. Shruthi, B. Vibha, B.A. Ashok Reddy, T.K. Kundu, C. Narayana, J. Phys. Chem. C 111 (2007) 4388.